Fast and Simple Au^{3+} Colorimetric Detection Using AgNPs and Investigating Its Reaction Mechanism

Faathir Al Faath Rachmawati, Bambang Rusdiarso, and Eko Sri Kunarti*

Department of Chemistry, Faculty of Mathematics and Natural Sciences, Universitas Gadjah Mada, Sekip Utara, Yogyakarta 55281, Indonesia

*** Corresponding author:**

email: eko_kunarti@ugm.ac.id

Received: May 15, 2023
Accepted: October 17, 2023

DOI: 10.22146/ijc.84446

Abstract: *One of the precious metals that has numerous applications is gold. Although it is non-toxic and biocompatible, the oxidized form, Au^{3+}, is toxic and can cause damage to human organs. Detection of Au^{3+} becomes a necessary and interesting topic to be conducted. Colorimetric analysis using metal nanoparticles such as silver nanoparticles (AgNPs) can analyze metal ions more simply, sensitively, and selectively than traditional methods. In this research, AgNPs were synthesized using polyvinyl alcohol (PVA) and ascorbic acid as stabilizers and reducing agents. The interaction between Au^{3+} and AgNPs selectively decreased the absorbance intensity of AgNPs and altered the color of colloidal AgNPs from yellow to colorless. These two phenomena indicated a redox reaction between Au^{3+} and AgNPs, leading to the decomposition of AgNPs. The decomposition of AgNPs (the proposed mechanism) was confirmed by TEM images and UV-vis spectra. The decrease in AgNPs' absorbance intensity correlated linearly with the increase in added Au^{3+} concentration. The calibration curve of ΔA versus Au^{3+} ion concentration yielded LOD and LOQ of 0.404 and 1.347 μg/mL, respectively.*

Keywords: *ascorbic acid; Au^{3+}; colorimetry; polyvinyl alcohol; silver nanoparticles*

■ INTRODUCTION

Gold is one of the precious metals that is often used in jewelries, electronic components, electrical equipments, and automotive applications [1]. As nanoparticles, gold also has wide applications in the fields of the environment, energy, and biosensors [2]. Moreover, gold nanoparticles can be used in the treatment of several diseases, such as rheumatoid arthritis, AIDS, malaria, tuberculosis, and cancer [3]. Although gold is biocompatible and non-toxic, the oxidized form of gold (Au^{3+}) is toxic. Au^{3+} ions can bind to DNA, proteins, and enzymes in the human body to form complexes that can cause damage to the liver, kidneys, and nervous system [4-5].

Au^{3+} detection can be carried out using analytical methods such as atomic absorption spectrometry [6], inductively coupled plasma atomic emission spectrometry [7], and inductively coupled plasma mass spectrometry [8]. Although these methods are sensitive, they require a long time to prepare samples, expensive instrumentation, and skilled labor. Colorimetric analysis using silver nanoparticles (AgNPs) can analyze metal ions more simply, sensitively, and selectively [9-10].

One of the inexpensive, simple, and easy methods for synthesizing AgNPs is chemical reduction. The synthesis is based on the reduction of silver metal salts using reducing agents in a stabilizer medium. A reducing agent is needed to reduce Ag^{+} into AgNPs (Ag^{0}) [11]. The commonly used reducing agents are citric acid, ascorbic acid, sodium borohydride, and block copolymers [12]. Roto et al. [13] have conducted research on the effect of reducing agents on the chemical and physical properties of AgNPs. The results showed that AgNPs synthesized with ascorbic acid had better uniformity in shape, size, and stability compared to AgNPs synthesized with other reducing agents such as sodium borohydride, trisodium citrate, hydrazine hydrate, and glucose.

AgNPs have been used frequently in colorimetric heavy metal detection with good selectivity and

sensitivity, including phenylbenzotriazole functionalized AgNPs (PBT-AgNPs) for the detection of Cr^{3+} [14], amino acid-based phenolic ligand functionalized AgNPs for the detection of Cd^{2+}, Hg^{2+} and Pb^{2+} [15], phenolic capping AgNPs for the detection of Ni^{2+} and Cd^{2+} [16], starch-stabilized AgNPs for the detection of Cr^{6+} [17], and *Bauhinia variegata* L. fabricated AgNPs for the detection of Hg^{2+} and Fe^{3+} [18]. However, research on the detection of Au^{3+} using AgNPs has not been widely reported. Only a few have been reported, such as *N*-deconyltromethamine functionalized AgNPs (based on the galvanic displacement of AgNPs) [19] and carboxymethyl cellulose stabilized AgNPs (based on the deposition of gold nanoparticles) [20]. The utilization of polyvinyl alcohol (PVA) as a stabilizer and ascorbic acid as a reducing agent in synthesizing AgNPs to detect Au^{3+} has not been reported until today. According to Guo et al. [21], PVA can stabilize AgNPs through chemical adsorption and steric effects. In this research, AgNPs were synthesized using ascorbic acid and PVA to detect Au^{3+}. The effects of pH, the addition of other cations, and Au^{3+} concentration were also evaluated in this study. The stability, shape, size, and crystal purity of the synthesized AgNPs were studied using UV-vis spectrophotometer, transmission electron microscope (TEM), and *X*-ray diffractometer (XRD).

■ EXPERIMENTAL SECTION

Materials

Silver nitrate, PVA, ascorbic acid, HCl, NaOH, $H[AuCl_4]$ and other salts (containing metal ions of Ca^{2+}, Cr^{6+}, Mg^{2+}, Cu^{2+}, Na^{+}, Hg^{2+}, Fe^{3+}, and Zn^{2+}) were purchased from Merck. All chemicals were analytical grade with no further purification and were prepared with double-distilled water.

Instrumentation

Samples were characterized by UV-vis spectrophotometer (Thermo Scientific Genesys 10S) to obtain UV-vis spectra. TEM images were captured using JEOL JEM-1400 while the Shimadzu XRD-6000 was used to examine the AgNPs crystal structure. All characterizations were conducted at room temperature.

Procedure

Synthesis and characterization of AgNPs

A 0.2 (w/v) % PVA solution as a stabilizer was prepared by heating and stirring using a hot plate magnetic stirrer. Meanwhile, a 3.0×10^{-4} M $AgNO_3$ solution as a silver precursor was prepared at room temperature. The synthesis was started by stirring and heating a 25 mL PVA solution to 80 °C and then the same volume of $AgNO_3$ solution was added dropwise. The temperature of the solution was kept at 80 °C. After the added $AgNO_3$ solution was used up, 1 mL of 0.1 M NaOH solution was slowly dropped, followed by 1.5 mL of 3×10^{-3} M ascorbic acid. The formation of AgNPs can be observed by the color change of the solution from colorless to yellow. The synthesized colloidal AgNPs were characterized by UV-vis spectrophotometer and TEM. While the characterization using XRD was carried out on solid AgNPs. The AgNPs were separated using a refrigerated high-speed centrifuge at 20,000 rpm for 20 min. The precipitate was dried in an oven at 70 °C for 24 h.

Effect of pH on the addition of Au^{3+} in AgNPs

The synthesized colloidal AgNPs were diluted to 5 μg/mL. Then, a series of 3 mL AgNPs was introduced by 0.1 M HCl or 0.1 M NaOH to adjust the pH to 2, 3, 4, 5, 6, 7, 8, 9, 10, 11, and 12. A 2 mL of 3 μg/mL Au^{3+} standard solution was added to each pH and reacted for 15 min. Each solution was analyzed by UV-vis spectrophotometer at 300–800 nm.

Effect of the addition of other cations

A series of 2 mL of standard solutions containing 3 g/mL Ca^{2+}, Cr^{6+}, Mg^{2+}, Cu^{2+}, Na^{+}, Hg^{2+}, Fe^{3+}, and Zn^{2+} was added to a series of 3 mL of 5 μg/mL AgNPs. The reaction was conducted for 15 min without pH adjustment. Each solution was analyzed by UV-vis spectrophotometer at 300–800 nm.

Effect of the addition of Au^{3+} at various concentrations

A series of Au^{3+} solutions were prepared at 0.2, 0.4, 0.6, 0.8, 1.0, 1.2, 1.4, 1.6, 1.8, 2.0, 2.2, 2.4, 2.6, 2.8, and 3.0 μg/mL. Each of the solutions was reacted with 3 mL

of 5 µg/mL AgNPs for 15 min and analyzed by UV-vis spectrophotometer at 300–800 nm.

Determination of limit of detection (LOD) and limit of quantification (LOQ)

The data required for the determination of LOD and LOQ were the absorbance of AgNPs after the addition of Au^{3+} ions at various concentrations of 0.02, 0.07, 0.08, 0.09, 0.15, 0.20, 0.40, 0.60, 0.80, 1.00, 1.20, 1.40, 1.60, 1.80, 2.00, 2.20, 2.40, 2.60, 2.80, and 3.00 µg/mL. The calibration curve was constructed with the data of various Au^{3+} concentrations versus ΔAbs of AgNPs. The LOD and LOQ were obtained statistically using the calibration curve. LOD and LOQ can be calculated by 3SD/b and 10SD/b, where SD is the standard deviation and b is the slope of the calibration curve.

■ RESULTS AND DISCUSSION

The synthesized AgNPs in this study have a yellow color with a maximum absorption wavelength of 402 nm (Fig. 1: 1st week). Fig. 1 shows the UV-vis spectra of freshly prepared AgNPs (1st week) and after 7 weeks. It can be observed that there was only a slight decrease in the absorbance peak at the maximum wavelength. No peak shifts or new peaks appeared on the UV-vis spectra. This indicates that the synthesized AgNPs are stable. Stability over time is important to ensure the usage of stored AgNPs.

The formation of UV-vis peaks between 390 and 410 nm indicates the presence of nanosized and spherical-shaped AgNPs [22]. Meanwhile, according to Mulfinger et al. [23], the maximum absorption wavelength can be used to predict particle size. AgNPs with maximum absorption wavelengths of around 395 to 420 nm have particle sizes of 10–35 nm. In this research, the absorption peak only has one slender main peak. This indicates that AgNPs have been formed with good shape uniformity [22].

The TEM image of synthesized AgNPs is presented in Fig. 2. The synthesized AgNPs are spherical and dispersed. This proves that PVA can stabilize AgNPs and prevent aggregation. Fig. 2 also shows the histogram of the particle size distribution of the synthesized AgNPs. The particle size of the AgNPs is in the range of 12 to 26 nm.

The XRD diffractogram of synthesized AgNPs can be seen in Fig. 3. Besides proving the formation of Ag^0

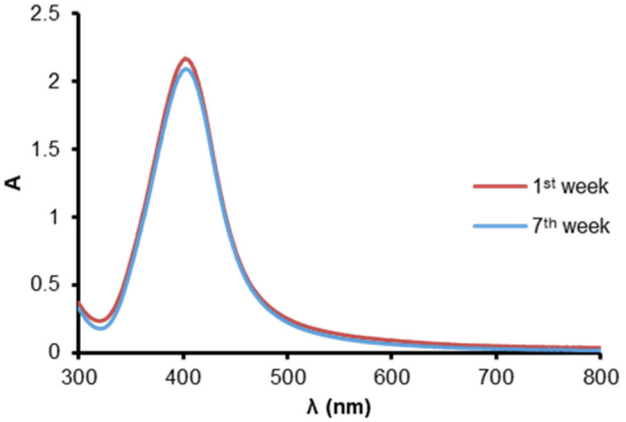

Fig 1. The UV-vis spectra of freshly prepared AgNPs and after 7 weeks

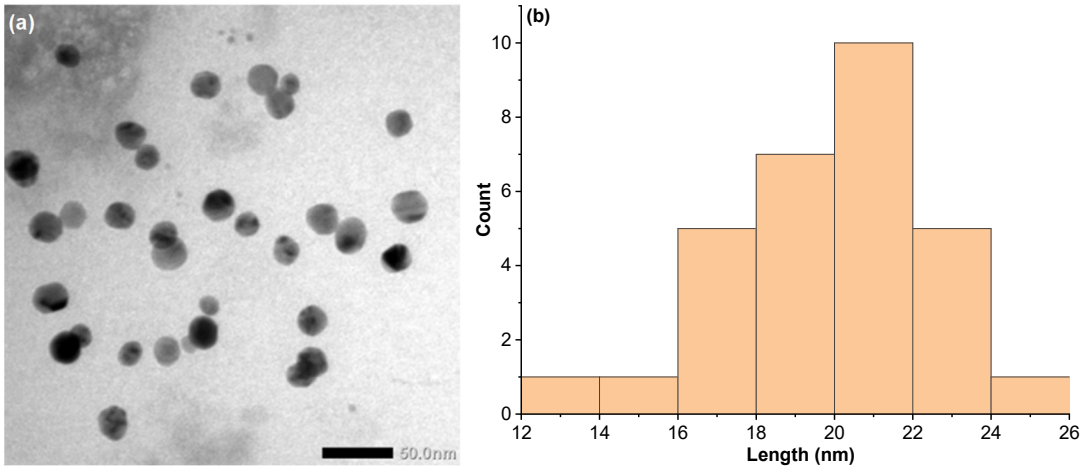

Fig 2. (a) TEM image and (b) particle size distribution of synthesized AgNPs

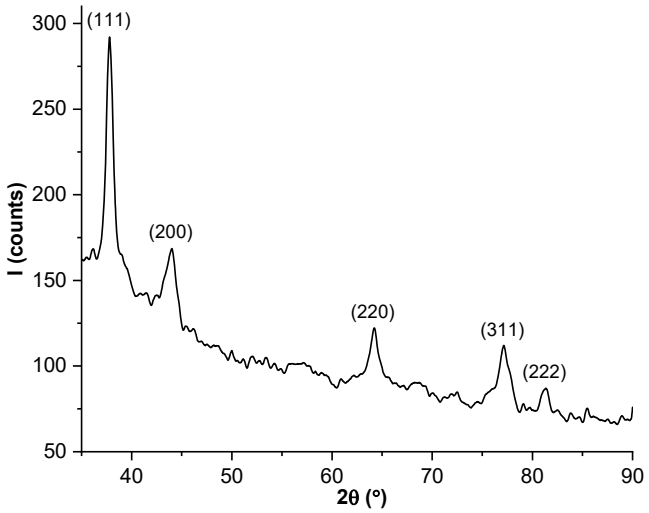

Fig 3. The XRD diffractogram of synthesized AgNPs

particles, characterization using XRD is important to understand the character, phase, and purity of synthesized crystals [24]. The 2θ peaks appear successively at angles of 37.8°, 43.9°, 64.2°, 77.1°, and 81.3°, which correspond to the Miller indices (111), (200), (220), (311), and (222). This XRD pattern agrees with the JCPDS data of pure Ag crystals (JCPDS No. 04-783). This indicates that Ag^0 had been successfully synthesized, and no another crystalline phase was found as an impurity. The synthesized AgNPs have a face-centered cubic (fcc) crystal structure with a lattice parameter value of 4.11 Å. The obtained parameter lattice is not much different from the reference (JCPDS No. 04-783).

The study of the effect of other cations in this research aims to determine the interference of other cations commonly found in water. The cations tested in this study were Ca^{2+}, Cr^{6+}, Mg^{2+}, Cu^{2+}, Na^{+}, Hg^{2+}, Fe^{3+}, and Zn^{2+}. Fig. 4 shows that the addition of various cations decreased the AgNPs' absorbance. The largest decrease was observed when Au^{3+} was added (Fig. 5). The addition of other cations did not reduce AgNP's absorbance significantly. This proves that other cations do not interfere with Au^{3+} sensing using AgNPs.

Fig. 6 depicts the color change of colloidal AgNPs after the addition of Au^{3+}. The color of colloidal AgNPs turned from yellow to colorless. The addition of other cations (Ca^{2+}, Cr^{6+}, Mg^{2+}, Cu^{2+}, Na^{+}, Hg^{2+}, Fe^{3+}, and Zn^{2+}) did not change the color of colloidal AgNPs.

The decrease of AgNPs' absorbance at 402 nm (λ_{max})

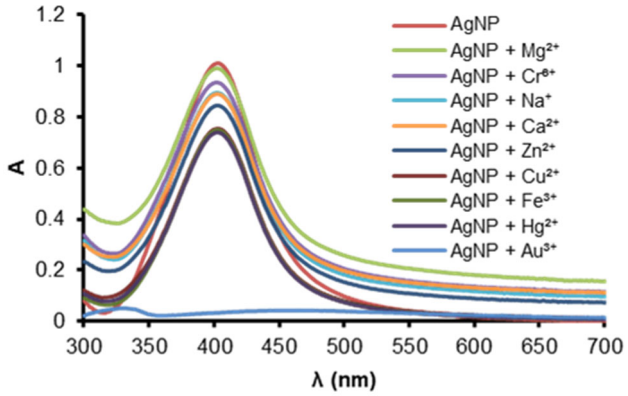

Fig 4. Combined UV-vis spectra of colloidal AgNPs before and after the addition of various cations at 3 µg/mL cation concentration

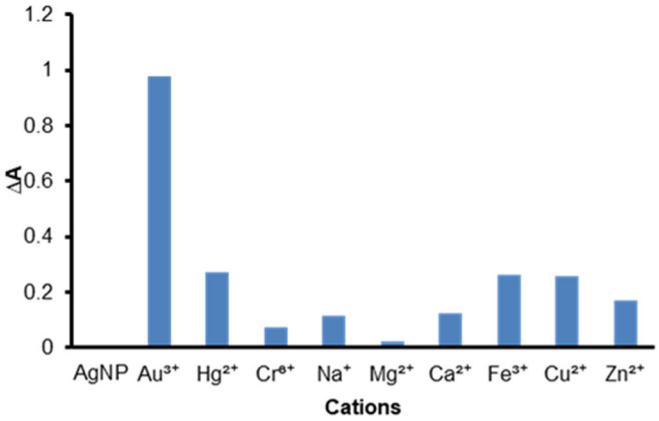

Fig 5. Combined ΔA of colloidal AgNPs after the addition of various cations

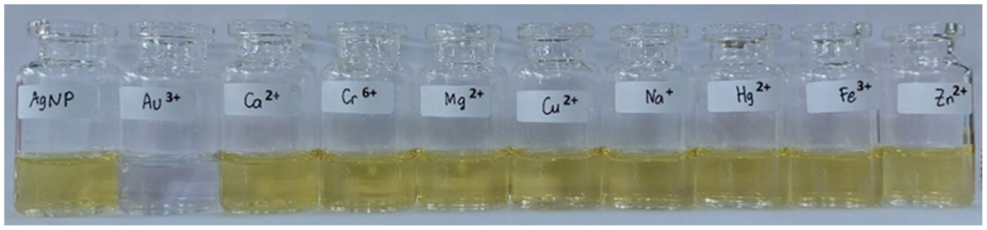

Fig 6. Photograph of initial AgNPs and with the presence of various cations

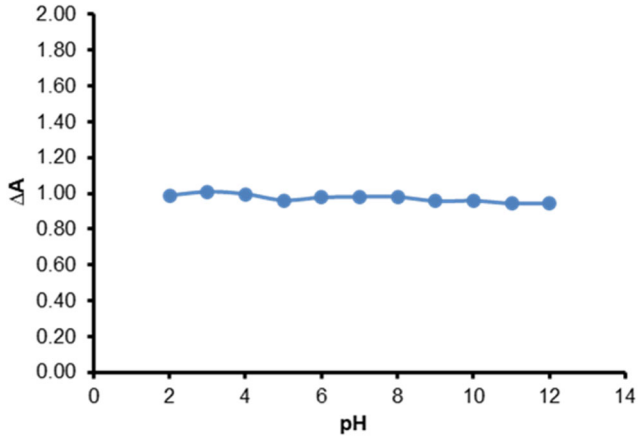

Fig 7. Effect of pH on the addition of Au^{3+} in AgNPs

on various pH is shown in Fig. 7. The graph clearly demonstrates that ΔA does not change with variations in pH. This suggests that the pH of the solution has no effect on the interaction of AgNPs with Au^{3+} ions.

Fig. 8 presents the UV-vis spectra of colloidal AgNPs in the presence of Au^{3+} at various concentrations (0–3 µg/mL). There is a correlation between the increase in Au^{3+} concentration and the decrease in AgNPs' absorbance at 402 nm (λ_{max}). The higher the Au^{3+} concentration, the greater the decrease in AgNPs' absorbance. Meanwhile, a relationship between the color alteration of colloidal AgNPs and the Au^{3+} concentration can be seen in Fig. 9. The photo displays that the higher the Au^{3+} concentration, the clearer the color alteration of colloidal AgNPs from yellow to colorless.

The relationship between the increase in Au^{3+} concentration and the decrease in AgNPs' absorbance at 402 nm (λ_{max}) is quantified in Fig. 10. The calibration

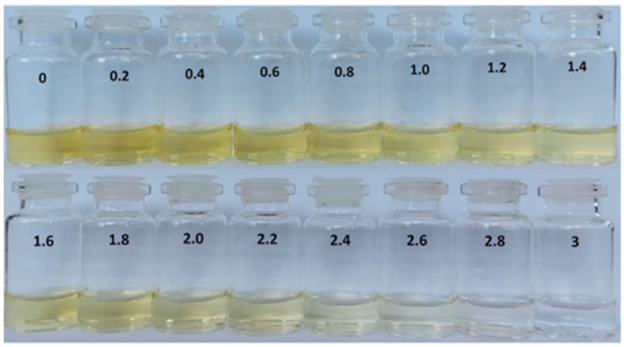

Fig 9. Photograph of colloidal AgNPs after adding Au^{3+} at various concentrations (0–3 µg/mL)

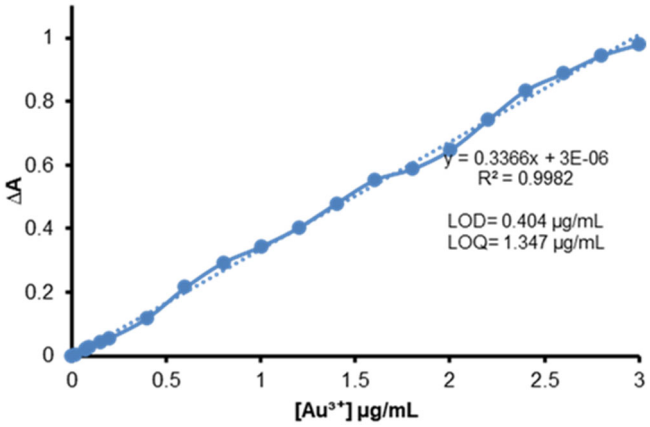

Fig 10. Calibration curve of colorimetric Au^{3+} sensing in the concentration range of 0–3 µg/mL

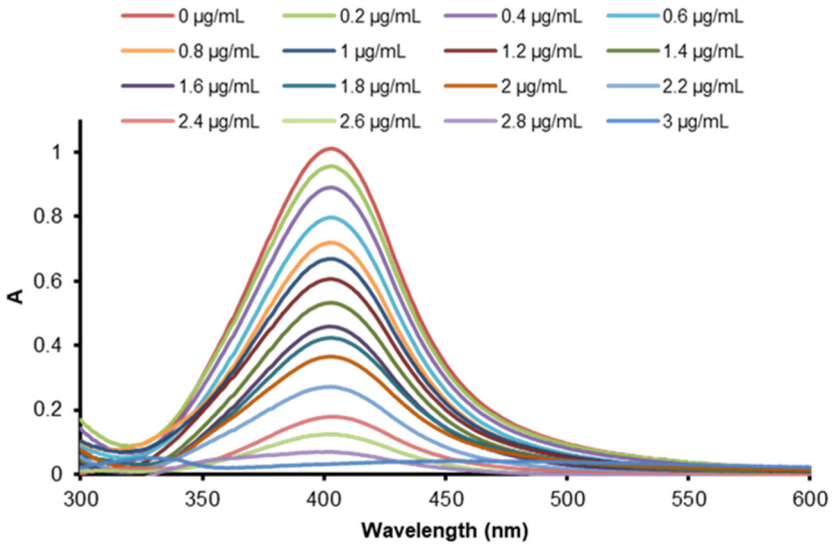

Fig 8. Effect of the concentration of Au^{3+} on the absorption intensity of AgNPs

curve demonstrates the linearity of this analysis. The linearity confirms that AgNPs can be used to detect Au^{3+} quantitatively using spectrophotometry. The calibration curve was used to statistically calculate the LOD and LOQ. The LOD is the lowest analyte concentration that can be distinguished from the assay background, while the LOQ is the lowest concentration at which the analyte can be quantitated at defined levels of imprecision and accuracy (bias) [25]. LOD and LOQ values obtained in this research are 0.404 and 1.347 µg/mL, respectively.

The mechanism of colorimetric analysis can be studied by observing the LSPR absorbance and color alteration of colloidal AgNPs after the addition of certain analytes [26]. In this research, the LSPR absorbance of AgNPs at 402 nm decreased in the presence of Au^{3+}, and the color of colloidal AgNPs turned from yellow to colorless. These two phenomena are frequently reported in the mechanism of AgNPs decomposition [27-29].

The simplified schematic of the proposed reaction mechanism is shown in Fig. 11. Part A is the silver ion-PVA complex. This complex was then reduced at 80 °C by ascorbic acid to form part B, or AgNPs. The yellow AgNPs then turned colorless (part C) after the addition of Au^{3+} ions. The changes from part B to part C occurred through the decomposition process of AgNPs. The results of the decomposition of AgNPs were silver ion-PVA complex or dissolved silver ions. Treatment with heating and the addition of ascorbic acid can change part C to part D or silver nanoparticles, which were indicated by the formation of light-yellow colloids.

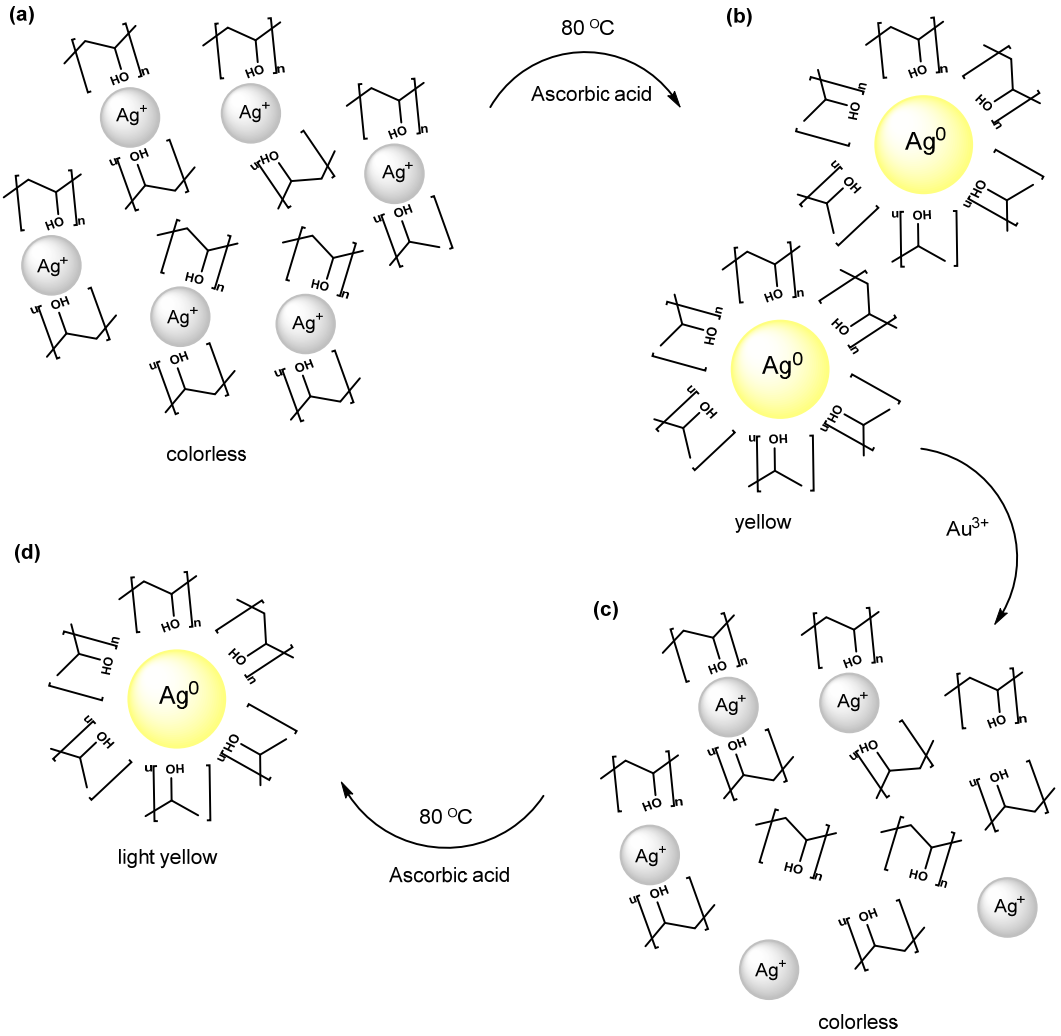

Fig 11. The simplified schematic of the proposed reaction mechanism

The decomposition of AgNPs is caused by a redox reaction between Au^{3+} and Ag^0. This is possible because the potential reduction of Au^{3+} is relatively high (+ 1.40 V). The potential reduction of Au^{3+} enables a positive E^0_{cell} reaction between Au^{3+} and Ag^0 (Eq. (1)). While other cations like Mg^{2+} or Na^+ cause negative E^0_{cell} reactions with Ag^0 (Eq. (2) and (3)). Positive E^0_{cell} reactions are more favorable than negative E^0_{cell} reactions. This explains why changes in the optical properties of AgNPs (the decrease in LSPR absorbance in Fig. 4 and the color alteration of colloidal AgNPs in Fig. 6) only happened with the addition of Au^{3+}.

$$3Ag + Au^{3+} \rightarrow 3Ag^+ + Au \qquad E^0_{cell} = 3.80\ V \qquad (1)$$

$$2Ag + Mg^{2+} \rightarrow 2Ag^+ + Mg \qquad E^0_{cell} = -0.77\ V \qquad (2)$$

$$Ag + Na^+ \rightarrow Ag^+ + Na \qquad E^0_{cell} = -1.91\ V \qquad (3)$$

The decomposition of AgNPs in this research has been ensured by characterization using TEM. Fig. 12 displays TEM images of the AgNPs before and after the addition of Au^{3+}. It can be seen that the size of AgNP decreased with the addition of Au^{3+}. May and Oluwafemi [30] attribute this to an oxidation reaction between AgNPs and cations, which causes the AgNPs to oxidize and smaller AgNPs to form. This was confirmed by the shift of the main peak of AgNPs from 402 to 330 nm after the addition of Au^{3+} (Fig. 4). The shifting of the AgNPs peak towards shorter wavelengths, also known as the blueshift of the surface plasmon resonance in AgNPs, indicates the decrease in the size of the AgNPs [31-32]. Furthermore, the number of AgNPs declined (parts a, c), and the spherical shape of AgNPs deformed (parts b, d). These two phenomena also affirm the proposed mechanism (AgNP decomposition).

The next investigation of the proposed mechanism was carried out by heating and adding ascorbic acid (AA) to added Au^{3+} AgNPs (AgNPs + Au^{3+}). With the assumption that a trace amount of silver ion-PVA complex remained after the addition of Au^{3+}, the process of heating and adding would trigger the formation of AgNPs. Fig. 13(a) depicts the color alteration of AgNPs + Au^{3+} from colorless to light yellow (lighter than initial AgNPs). While combined UV-vis spectra (Fig. 13(b)) show an emerging new peak at 416 nm.

The formation of light-yellow colloids indicated the presence of AgNPs, confirmed by an emerging peak at 416 nm. The color is lighter, and the intensity of peak absorption is lower than the initial AgNPs. These suggested that fewer AgNPs formed than the initial AgNPs. Meanwhile, the broadening and shifting of

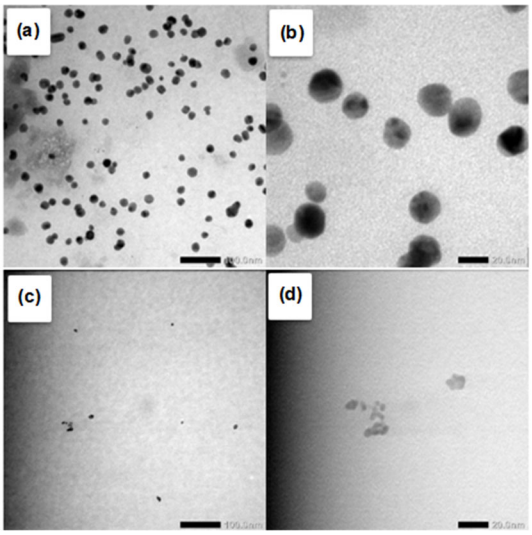

Fig 12. TEM images of initial AgNPs at (a) 100 nm scale, (b) 20 nm scale, and added Au^{3+} to AgNPs at (c) 100 nm scale, (d) 20 nm scale

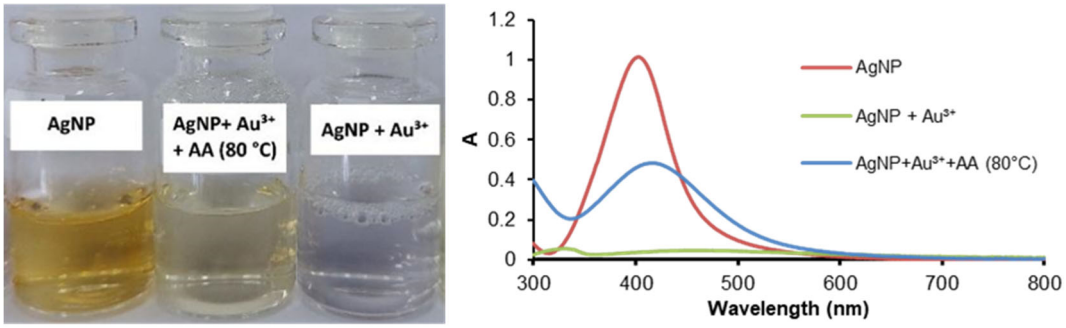

Fig 13. (a) Photograph and (b) combined UV-vis spectra of AgNPs, AgNP + Au^{3+}, and AgNP + Au^{3+} + AA (80 °C)

absorbance wavelength from 402 to 416 indicated that bigger and more varied-sized AgNPs had been formed. These are possible since the initial AgNPs had been synthesized in a controlled system (silver ion-PVA complex), while the AgNP + Au^{3+} + AA (80 °C) (light yellow colloid) was formed in an uncontrolled system resulting from AgNP decomposition.

CONCLUSION

The results showed that PVA could be used as a stabilizer and ascorbic acid as a reducing agent in the synthesis of AgNPs. AgNPs were successfully synthesized with a spherical shape, stability over time, and size in the range of 12–26 nm. The absorbance peak of AgNPs at λ_{max} 402 nm was only affected by the addition of Au^{3+} ions, while other cations and the pH of the solution had no significant effect on the absorbance of AgNPs. The absorbance of colloidal AgNPs decreased as the concentration of Au^{3+} ions was increased. The calibration curve of ΔA versus Au^{3+} ion concentration yielded LOD and LOQ at 0.404 and 1.347 μg/mL, respectively. The proposed mechanism is the decomposition of AgNPs due to a redox reaction between Ag^0 and Au^{3+}, which can be seen from the color change of colloidal AgNPs from yellow to colorless.

ACKNOWLEDGMENTS

The authors acknowledge the Faculty of Mathematics and Natural Sciences, Universitas Gadjah Mada, for the financial support of this research (DAMAS 2023 internal research grant, with contract number: 51/UN1/FMIPA.1.3/KP/PT.01.03/2023).

AUTHOR CONTRIBUTIONS

Eko Sri Kunarti: Conception and design of study, acquisition of data, analysis and interpretation of data, drafting the manuscript, Faathir Al Faath Rachmawati: Conception and design of study, acquisition of data, analysis and interpretation of data, drafting the manuscript, revising the manuscript critically for important intellectual content, Bambang Rusdiarso: Conception and design of study, acquisition of data.

REFERENCES

[1] Corti, C.W., Holliday, R.J., and Thompson, D.T., 2002, Developing new industrial applications for gold: Gold nanotechnology, *Gold Bull.*, 35 (4), 111–117.

[2] Hassan, H., Sharma, P., Hasan, M.R., Singh, S., Thakur, D., and Narang, J., 2022, Gold nanomaterials – The golden approach from synthesis to applications, *Mater. Sci. Energy Technol.*, 5, 375–390.

[3] Vines, J.B., Yoon, J.H., Ryu, N.E., Lim, D.J., and Park, H., 2019, Gold nanoparticles for photothermal cancer therapy, *Front. Chem.*, 7, 167.

[4] Li, X., Hu, Q., Yang, K., Zhao, S., Zhu, S., Wang, B., Zhang, Y., Yi, J., Song, X., and Lan, M., 2022, Red fluorescent carbon dots for sensitive and selective detection and reduction of Au^{3+}, *Sens. Actuators, B*, 371, 132534.

[5] Yang, Y.H., Tao, X., Bao, Q.L., Yang, J., Su, L.J., Zhang, J.T., Chen, Y., and Yang, L.J., 2023, A highly selective supramolecular fluorescent probe for detection of Au^{3+} based on supramolecular complex of pillar[5]arene with 3,3'-dihydroxybenzidine, *J. Mol. Liq.*, 370, 121018.

[6] Afzali, D., Daliri, Z., and Taher, M.A., 2014, Flame atomic absorption spectrometry determination of trace amount of gold after separation and preconcentration onto ion-exchange polyethylenimine coated on Al_2O_3, *Arabian J. Chem.*, 7 (5), 770–774.

[7] Zari, N., Hassan, J., Tabar-Heydar, K., and Ahmadi, S.H., 2020, Ion-association dispersive liquid-liquid microextraction of trace amount of gold in water samples and ore using Aliquat 336 prior to inductivity coupled plasma atomic emission spectrometry determination, *J. Ind. Eng. Chem.*, 86, 47–52.

[8] Malejko, J., Świerżewska, N., Bajguz, A., and Godlewska-Żyłkiewicz, B., 2018, Method development for speciation analysis of nanoparticle and ionic forms of gold in biological samples by

high performance liquid chromatography hyphenated to inductively coupled plasma mass spectrometry, *Spectrochim. Acta, Part B*, 142, 1–7.

[9] Loiseau, A., Asila, V., Aullen, G.B., Lam, M., Salmain, M., and Boujday, S., 2019, Silver-based plasmonic nanoparticles for and their use in biosensing, *Biosensors*, 9 (2), 78.

[10] Ebralidze, I.I., Laschuk, N.O., Poisson, J., and Zenkina, O.V., 2019, *Nanomaterials Design for Sensing Applications*, Elsevier, Amsterdam, Netherlands.

[11] Quintero-Quiroz, C., Acevedo, N., Zapata-Giraldo, J., Botero, L.E., Quintero, J., Zárate-Triviño, D., Saldarriaga, J., and Pérez, V.Z., 2019, Optimization of silver nanoparticle synthesis by chemical reduction and evaluation of its antimicrobial and toxic activity, *Biomater. Res*., 23 (1), 27.

[12] Nie, P., Zhao, Y., and Xu, H., 2023, Synthesis, applications, toxicity and toxicity mechanisms of silver nanoparticles: A review, *Ecotoxicol. Environ. Saf*., 253, 114636.

[13] Roto, R., Rasydta, H.P., Suratman, A., and Aprilita, N.H., 2018, Effect of reducing agents on physical and chemical properties of silver nanoparticles, *Indones. J. Chem*., 18 (4), 614–620.

[14] Qadri, T., Khan, S., Begum, I., Ahmed, S., Shah, Z.A., Ali, I., Ahmed, F., Hussain, M., Hussain, Z., Rahim, S., and Shah, M.R., 2022, Synthesis of phenylbenzotriazole derivative stabilized silver nanoparticles for chromium(III) detection in tap water, *J. Mol. Struct*., 1267, 133589.

[15] Vinod Kumar, V., and Anthony, S.P., 2014, Silver nanoparticles based selective colorimetric sensor for Cd^{2+}, Hg^{2+} and Pb^{2+} ions: Tuning sensitivity and selectivity using co-stabilizing agents, *Sens. Actuators, B*, 191, 31–36.

[16] Ebrahim Mohammadzadeh, S., Faghiri, F., and Ghorbani, F., 2022, Green synthesis of phenolic capping AgNPs by green walnut husk extract and its application for colorimetric detection of Cd^{2+} and Ni^{2+} ions in environmental samples, *Microchem. J*., 179, 107475.

[17] Sapyen, W., Toonchue, S., Praphairaksit, N., and Imyim, A., 2022, Selective colorimetric detection of Cr(VI) using starch-stabilized silver nanoparticles and application for chromium speciation, *Spectrochim. Acta, Part A*, 274, 121094.

[18] Kumar Chandraker, S., Kumar Ghosh, M., Parshant, P., Tiwari, A., Kumar Ghorai, T., and Shukla, R., 2022, Efficient sensing of heavy metals (Hg^{2+} and Fe^{3+}) and hydrogen peroxide from *Bauhinia variegata* L. fabricated silver nanoparticles, *Inorg. Chem. Commun.*, 146, 110173.

[19] Megarajan, S., Kamlekar, R.K., Kumar, P.S., and Anbazhagan, V., 2019, Rapid and selective colorimetric sensing of Au^{3+} ions based on galvanic displacement of silver nanoparticles, *New J. Chem.*, 43 (47), 18741–18746.

[20] Jayeoye, T.J., Supachettapun, C., and Muangsin, N., 2023, Ascorbic acid supported carboxymethyl cellulose stabilized silver nanoparticles as optical nanoprobe for Au^{3+} detection in environmental sample, *Arabian J. Chem.*, 16 (4), 104552.

[21] Guo, G., Gan, W., Luo, J., Xiang, F., Zhang, J., Zhou, H., and Liu, H., 2010, Preparation and dispersive mechanism of highly dispersive ultrafine silver powder, *Appl. Surf. Sci.*, 256 (22), 6683–6687.

[22] Guzmán, K., Kumar, B., Grijalva, M., Debut, A., and Cumbal, L., 2022, "Ascorbic Acid-assisted Green Synthesis of Silver Nanoparticles: pH and Stability Study" in *Green Chemistry – New Perspectives*, Eds. Kumar, B., and Debut, A., IntechOpen, Rijeka, Croatia.

[23] Mulfinger, L., Solomon, S.D., Bahadory, M., Jeyarajasingam, A.V., Rutkowsky, S.A., and Boritz, C., 2007, Synthesis and study of silver nanoparticles, *J. Chem. Educ.*, 84 (2), 322.

[24] Khan, I., Saeed, K., and Khan, I., 2019, Nanoparticles: Properties, applications and toxicities, *Arabian J. Chem.,* 12 (7), 908–931.

[25] Nair, H., and Clarke, W., 2017, *Mass Spectrometry for the Clinical Laboratory*, Academic Press, Cambridge, US.

[26] Prosposito, P., Burratti, L., and Venditti, I., 2020, Silver nanoparticles as colorimetric sensors for water pollutants*, Chemosensors*, 8 (2), 26.

[27] Gao, X., Lu, Y., He, S., Li, X., and Chen, W., 2015,

Colorimetric detection of iron ions(III) based on the highly sensitive plasmonic response of the *N*-acetyl-L-cysteine-stabilized silver nanoparticles, *Anal. Chim. Acta*, 879, 118–125.

[28] Bhattacharjee, Y., and Chakraborty, A., 2014, Label-free cysteamine-capped silver nanoparticle-based colorimetric assay for Hg(II) detection in water with subnanomolar exactitude, *ACS Sustainable Chem. Eng.*, 2 (9), 2149–2154.

[29] Ahmed, F., Kabir, H., and Xiong, H., 2020, Dual colorimetric sensor for Hg^{2+}/Pb^{2+} and an efficient catalyst based on silver nanoparticles mediating by the root extract of *Bistorta amplexicaulis*, *Front. Chem.*, 8, 591958.

[30] May, B.M.M., and Oluwafemi, O.S., 2016, Sugar-reduced gelatin-capped silver nanoparticles with high selectivity for colorimetric sensing of Hg^{2+} and Fe^{2+} ions in the midst of other metal ions in aqueous solutions, *Int. J. Electrochem. Sci.*, 11, 8096–8108.

[31] Raza, S., Yan, W., Stenger, N., Wubs, M., and Mortensen, N.A., 2013, Blueshift of the surface plasmon resonance in silver nanoparticles: Substrate effects, *Opt. Express*, 21 (22), 27344–27355.

[32] Roddu, A.K., Wahab, A.W., Ahmad, A., and Taba, P., 2019, Green-route synthesis and characterization of the silver nanoparticles resulted by bio-reduction process, *J. Phys.: Conf. Ser.*, 1341 (3), 032004.